Examination of the different roles of neutron transfer in the sub-barrier fusion reactions $^{32}S + ^{94,96}Zr$ and $^{40}Ca + ^{94,96}Zr$

V. V. Sargsyan,[1,2] G. G. Adamian,[1] N. V. Antonenko,[1] W. Scheid,[3] and H. Q. Zhang[4]
[1]*Joint Institute for Nuclear Research, 141980 Dubna, Russia*
[2]*Yerevan State University, M. Manougian 1, 0025, Yerevan, Armenia*
[3]*Institut für Theoretische Physik der Justus-Liebig-Universität, D-35392 Giessen, Germany*
[4]*China Institute of Atomic Energy, P.O. Box 275, Beijing 102413, China*
(Received 22 August 2014; revised manuscript received 10 December 2014; published 26 January 2015)

The sub-barrier capture (fusion) reactions $^{32}S + ^{90,94,96}Zr$, $^{36}S + ^{90,96}Zr$, $^{40}Ca + ^{90,94,96}Zr$, and $^{48}Ca + ^{90,96}Zr$ with positive and negative Q values for neutron transfer are studied with the quantum diffusion approach and the universal fusion function representation. For these systems, the s-wave capture probabilities are extracted from the experimental excitation functions and are also analyzed. Different effects of the positive Q_{xn}-value neutron transfer in the fusion enhancement are revealed in the relatively close reactions $^{32}S + ^{94,96}Zr$ and $^{40}Ca + ^{94,96}Zr$.

DOI: 10.1103/PhysRevC.91.014613 PACS number(s): 25.70.Jj, 24.10.−i, 24.60.−k

I. INTRODUCTION

The nuclear deformation effects are identified as playing a major role in the magnitude of the sub-barrier fusion (capture) cross sections [1,2]. There are several experimental evidences which confirm the straightforward influence of nuclear deformation on the fusion. If the target nucleus is prolate in the ground state, the Coulomb field on its tips is lower than on its sides. Thus, the capture or fusion probability increases at energies below the barrier corresponding to the spherical nuclei.

The dynamics of neutron-transfer-mediated sub-barrier capture and fusion has not yet been revealed [2]. The cross section enhancement in the sub-barrier fusion of $^{58}Ni + ^{64}Ni$, with respect to $^{58}Ni + ^{58}Ni$ [3], is interpreted in Ref. [4] as a kinematic effect due to the positive Q_{2n} value of the ground-state-to-ground-state two-neutron transfer ($2n$-transfer) channel. A correlation is observed between considerable sub-barrier fusion enhancement and positive Q_{xn} values for neutron transfer in the reactions $^{40}Ca + ^{94,96}Zr$ [5–7] and $^{40}Ca + ^{116,124,132}Sn$ [8,9].

The importance of neutron transfer with positive Q_{xn} values in nuclear fusion (capture) originates from the fact that neutrons are insensitive to the Coulomb barrier and their transfer starts at quite larger separations, before the projectile is captured by the target nucleus. It is generally thought that the sub-barrier capture (fusion) cross section increases because of the neutron transfer [5–20]. However, the reduced excitation functions for the reactions $^{16,17,18}O + ^{A}Sn$ ($A = 112$, 116–120, 122, 124) [21], scaled to remove the effects of smoothly varying barrier parameters, do not show any strong dependence on the mass number of the target or the projectile. The relative changes are within a factor of 2 and are not correlated with the positive Q_{xn} values of neutron-transfer channels in these reactions. As shown in Ref. [22], the neutron-transfer channels with positive Q_{xn} value weakly influence the capture (fusion) cross section in the $^{60}Ni + ^{100}Mo$ reaction at sub-barrier energies. In the reactions $^{40}Ca + ^{116,124}Sn$ ($Q_{2n} > 0$) and $^{132}Sn,^{130}Te + ^{58,64}Ni$ ($Q_{2n} > 0$) at energies above and a few MeV below the Coulomb barrier, the effect of transfer channels on the capture (fusion) is demonstrated to be very weak with no significant differences observed in the reduced excitation functions [8,23]. In comparison with the $^{16}O + ^{76}Ge$ reaction [24], the fusion enhancement due to the positive Q_{2n} value is not revealed in the $^{18}O + ^{74}Ge$ reaction.

It is presently not clear why the neutron transfers with positive Q_{xn} values play a decisive role in the fusion reactions $^{40}Ca + ^{48}Ca$, $^{58}Ni + ^{64}Ni$, $^{40}Ca + ^{94,96}Zr$, and $^{40}Ca + ^{116,124,132}Sn$ and weakly influence the fusion reactions $^{58,64}Ni + ^{132}Sn$, $^{58,64}Ni + ^{130}Te$, $^{60}Ni + ^{100}Mo$, $^{18}O + ^{74}Ge$, and $^{18}O + ^{A}Sn$ [2,25]. Although the enhancement appears to be related to the existence of large positive Q_{xn} values for neutron transfer, it is not proportional to the magnitudes of those Q_{xn} values, which are larger for $^{40}Ca + ^{96}Zr$ ($^{40}Ca + ^{132}Sn$ or $^{40}Ca + ^{124}Sn$) than for $^{40}Ca + ^{94}Zr$ ($^{40}Ca + ^{124}Sn$ or $^{40}Ca + ^{116}Sn$). The sub-barrier enhancements are similar in these reactions. So, the influence of neutron transfer on the capture process is not easily explained.

The quantum diffusion approach [26–30] was applied to study the role of neutron transfer with positive Q_{xn} value in the capture (fusion) reactions at sub-, near- and above-barrier energies. A good agreement of the theoretical calculations with the experimental data was demonstrated. As found, the change of the capture cross section after the neutron transfer occurs due to the change of the deformations of nuclei [26–30]. Thus, the effect of neutron transfer is an indirect influence of quadrupole deformation. As demonstrated in Ref. [27], neutron transfer can weakly influence or even suppress the capture (fusion) cross section in some reactions. Later similar conclusions were pointed out in Ref. [31].

Applying the quantum diffusion approach [26–30] (Sec. IV), the universal fusion function representation [32,33] (Sec. II), and capture probabilities extracted from experimental excitation functions (Sec. III), we try to answer the question of how neutron transfer influences the sub-barrier capture cross section in the reactions $^{32}S + ^{90,94,96}Zr$, $^{36}S + ^{90,96}Zr$, $^{40}Ca + ^{90,94,96}Zr$, and $^{48}Ca + ^{90,96}Zr$ at near and sub-barrier energies. We show why the influence of positive-Q_{xn}-value neutron transfer is completely different in the relatively close reactions $^{32}S + ^{94,96}Zr$ and $^{40}Ca + ^{94,96}Zr$.

II. EXPERIMENTAL REDUCED CAPTURE CROSS SECTIONS

To analyze the capture cross sections in the reactions with different Coulomb barrier heights V_b and radius R_b calculated in the case of spherical nuclei, it is useful to compare not the excitation functions, but the dependence of the dimensionless quantities $2E_{\rm c.m.}\sigma_{\rm cap}(E_{\rm c.m.})/(\hbar\omega_b R_b^2)$ versus $x = (E_{\rm c.m.} - V_b)/(\hbar\omega_b)$ or $(E_{\rm c.m.} - V_b)$ [32,33]. Here, ω_b and μ are the frequency of an inverted-oscillator-approximated barrier and the reduced mass of the system, respectively. In the reactions, where the capture and fusion cross sections coincide, the comparison of experimental data with the universal fusion function [32,33] allows us to conclude about the role of static deformations of the colliding nuclei and the nucleon transfer between them in the capture cross section. Indeed, the universal function disregards these effects. To extract the values of V_b, R_b, and ω_b (Table I), we calculate the nucleus-nucleus interaction potential. The same potential is used within the quantum diffusion approach [26–30] (see Sec. IV).

For the reactions ^{40}Ca + ^{90}Zr, ^{48}Ca + ^{90,96}Zr, and ^{36}S + ^{90,96}Zr, with almost spherical nuclei and without neutron transfer (the negative Q_{xn} values), the experimental cross sections are rather close and fall with almost the same rate as the universal fusion function (Fig. 1). For the reactions ^{40}Ca + ^{94,96}Zr with neutron transfer (the positive Q_{xn} values), one can clearly see that the reduced cross sections strongly deviate from those for the reactions ^{40}Ca + ^{90}Zr, ^{36}S + ^{90,96}Zr, ^{48}Ca + ^{90,96}Zr, where neutron transfer is suppressed.

In the reactions ^{32}S + ^{90,94,96}Zr with the strongly deformed projectile ^{32}S, the deviations of the reduced excitation functions from those in the reactions ^{36}S + ^{90,96}Zr (Fig. 1) are mainly caused by the static deformation effects. Despite the Q_{xn} values for the neutron transfer range from negative (^{32}S + ^{90}Zr)to large positive values (^{32}S + ^{94,96}Zr), the reduced capture (fusion) cross sections appear to be almost the same. So, we observe the strong and weak influence of neutron transfer on the capture cross sections in the reactions ^{40}Ca + ^{94,96}Zr and ^{32}S + ^{94,96}Zr, respectively. The universal fusion function is mainly shown to discriminate the reactions ^{40}Ca + ^{94,96}Zr with neutron transfer from the reactions ^{40}Ca + ^{90}Zr, ^{48}Ca + ^{90,96}Zr, and ^{36}S + ^{90,96}Zr without neutron transfer and to demonstrate the similarity of the fusion enhancements in the reactions ^{32}S + ^{94,96}Zr and ^{32}S + ^{90}Zr with and without, respectively, neutron transfer. The fusion enhancement or hindrance in these reactions can be studied by the calculation of the dynamic polarization potential including contributions from inelastic excitations and nucleon transfer [1,37–39].

TABLE I. The barrier parameters used in Fig. 1.

Reactions	V_b (MeV)	R_b (fm)	$\hbar\omega_b$ (MeV)
^{32}S + ^{90}Zr	79.6	11.1	3.35
^{32}S + ^{94}Zr	77.0	11.2	3.35
^{32}S + ^{96}Zr	76.5	11.3	3.36
^{36}S + ^{90}Zr	77.2	11.3	3.22
^{36}S + ^{96}Zr	75.2	11.5	3.36
^{40}Ca + ^{90}Zr	96.2	11.3	3.34
^{40}Ca + ^{94}Zr	95.2	11.4	3.31
^{40}Ca + ^{96}Zr	94.2	11.5	3.25
^{48}Ca + ^{90}Zr	94.5	11.6	3.12
^{48}Ca + ^{96}Zr	92.9	11.7	3.07
^{40}Ca + ^{40}Ca	53.3	10.5	3.20

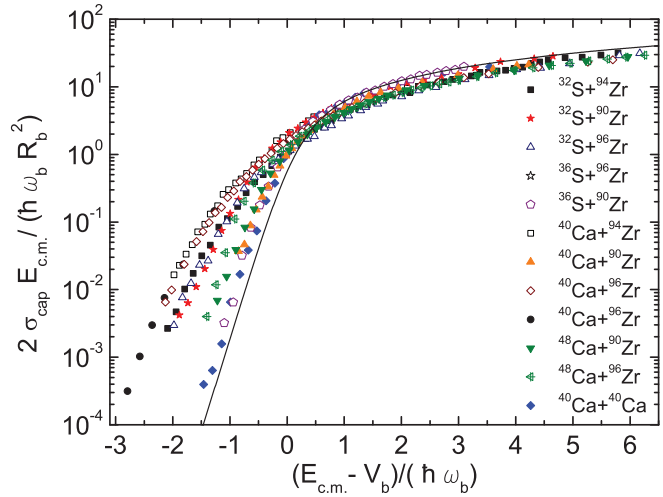

FIG. 1. (Color online) The experimental reduced fusion excitation functions $\frac{2E_{\rm c.m.}}{\hbar\omega_b R_b^2}\sigma_{\rm cap}(E_{\rm c.m.})$ (symbols) [5–7,18,20,34–36] and the universal fusion function $F_0 = \ln\{1 + \exp[2\pi(E_{\rm c.m.} - V_b)/(\hbar\omega_b)]\}$ (solid line) vs $\frac{E_{\rm c.m.}-V_b}{\hbar\omega_b}$ for the reactions indicated.

III. CAPTURE PROBABILITIES EXTRACTED FROM EXPERIMENTAL CAPTURE EXCITATION FUNCTIONS

Shifting the energy by the rotational energy $E_R(J) = \frac{\hbar^2 J(J+1)}{2\mu R_b^2}$ [40], one can approximate the angular momentum J dependence of the transmission (capture) probability $P_{\rm cap}(E_{\rm c.m.}, J)$ at a given $E_{\rm c.m.}$:

$$P_{\rm cap}(E_{\rm c.m.}, J) \approx P_{\rm cap}[E_{\rm c.m.} - E_R(J), J = 0]. \qquad (1)$$

If we use the formula for the capture cross section, convert the sum over the partial waves J into an integral, and express J by the variable $E = E_{\rm c.m.} - E_R(J)$, we obtain the following simple expression:

$$\sigma_{\rm cap}(E_{\rm c.m.}) = \frac{\pi R_b^2}{E_{\rm c.m.}} \int_0^{E_{\rm c.m.}} dE\, P_{\rm cap}(E, J = 0). \qquad (2)$$

Multiplying this equation by $E_{\rm c.m.}/(\pi R_b^2)$ and differentiating over $E_{\rm c.m.}$, one obtains [40]

$$P_{\rm cap}(E_{\rm c.m.}, J = 0) = \frac{1}{\pi R_b^2} \frac{d[E_{\rm c.m.}\sigma_{\rm cap}(E_{\rm c.m.})]}{dE_{\rm c.m.}}. \qquad (3)$$

One can see that $\frac{d[E_{\rm c.m.}\sigma_{\rm cap}(E_{\rm c.m.})]}{dE_{\rm c.m.}}$ has the meaning of the s-wave transmission in the entrance channel. Therefore, the s-wave capture probability can be extracted with satisfactory accuracy from the experimental capture cross sections $\sigma_{\rm cap}(E_{\rm c.m.})$ at energies near and below the Coulomb barrier. Note that at the energies considered the dependence of the Coulomb barrier radius on the angular momentum is very weak.

The extraction method just described requires some procedure to smooth the experimental data since the values of

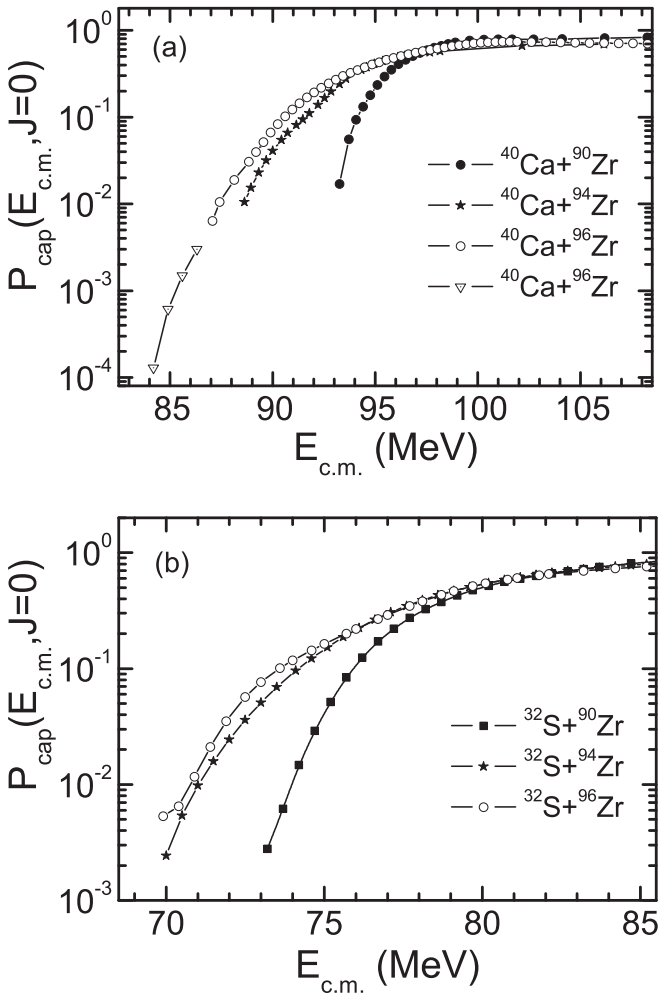

FIG. 2. The extracted s-wave capture probabilities for the reactions indicated by employing Eq. (3) (symbols connected by lines). The experimental capture (fusion) excitation functions used are from Refs. [5–7,18,20].

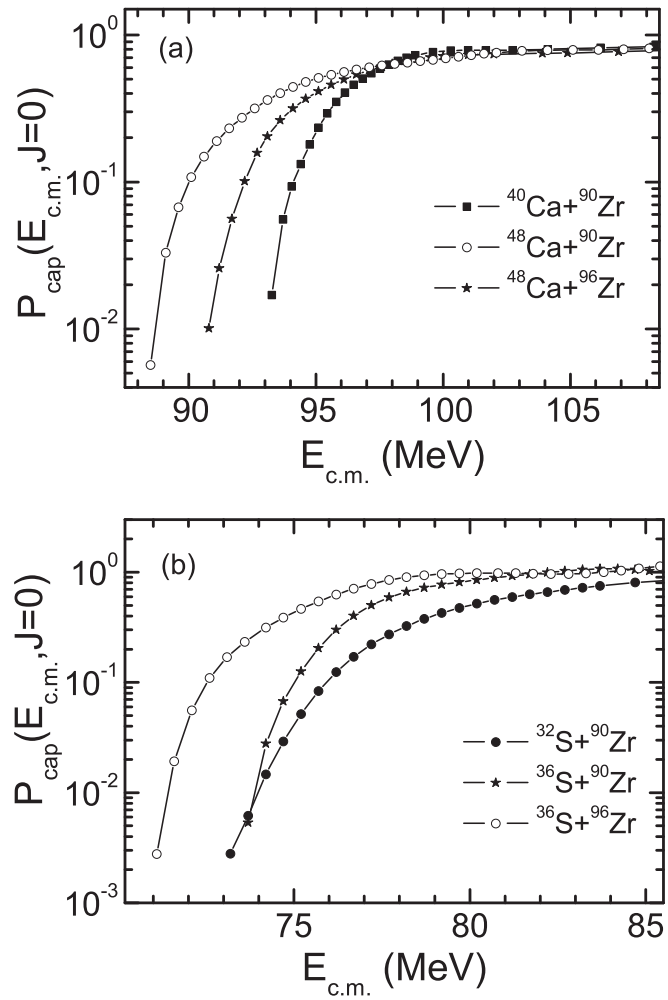

FIG. 3. The extracted s-wave capture probabilities for the reactions indicated by employing Eq. (3) (symbols connected by lines). The experimental capture (fusion) excitation functions used are from Refs. [5,18,34,35].

$E_{c.m.}\sigma_{cap}(E_{c.m.})$ have error bars. We spline the experimental points of $E_{c.m.}\sigma_{cap}(E_{c.m.})$ by the Bézier parametric curve [41].

In Figs. 2 and 3, the extracted capture probabilities $P_{cap}(E, J = 0)$ demonstrate the influence of nucleon transfer on the capture (fusion) excitation function. In the reactions $^{40}Ca + ^{90}Zr$ and $^{48}Ca + ^{90,96}Zr$ with the negative Q_{xn} values for nucleon transfer, the capture probability exhibits a steep falloff of the probability at low energies. However, the first derivatives of $P_{cap}(E, J = 0)$ are almost the same. Conversely, the reactions $^{40}Ca + ^{94,96}Zr$ have positive Q_{xn} values for neutron transfer. This leads to the smaller slope of probability functions at sub-barrier energies. The capture probabilities in the reactions $^{40}Ca + ^{94,96}Zr$ are close to each other.

Because the nucleus ^{36}S is spherical, the slopes of functions $P_{cap}(E, J = 0)$ for the reactions $^{36}S + ^{90,96}Zr$ are larger than those for the reactions $^{32}S + ^{94,96}Zr$ and $^{32}S + ^{90}Zr$ with the strongly deformed ^{32}S. The slopes of functions $P_{cap}(E, J = 0)$ are rather similar (Fig. 3) in the $^{32}S + ^{90}Zr$ reaction with the negative Q_{xn} values for neutron transfer and in the reactions $^{32}S + ^{94,96}Zr$ (Fig. 2) with the positive Q_{xn} values for neutron transfer. Thus, the enhancement of capture probability in these reactions has the same origin. It arises due to the large static deformations of nuclei $^{32,34}S$ and the neutron transfer is not responsible for the capture (fusion) enhancement.

As follows from the extracted capture probabilities, the experimental normalizations of the cross sections are different in the reactions $^{32}S + ^{90,94,96}Zr$ and $^{36}S + ^{90,96}Zr$. One should think about the experimental reasons for such deviations.

IV. CALCULATIONS WITHIN THE QUANTUM DIFFUSION APPROACH

In the quantum diffusion approach [26–30,42] the collisions of nuclei are described with a single relevant collective variable: the relative distance between the colliding nuclei. This approach takes into consideration the fluctuation and dissipation effects in collisions of heavy ions that model the coupling with various channels (for example, the noncollective single-particle excitations and low-lying collective dynamical modes of the target and the projectile). We have to mention

that many quantum-mechanical and non-Markovian effects accompanying the passage through the potential barrier are taken into consideration in our formalism [26–30,42]. The nuclear deformation effects are taken into account through the dependence of the nucleus-nucleus potential on the deformations and mutual orientations of the colliding nuclei. To calculate the nucleus-nucleus interaction potential $V(R)$, we use the procedure presented in Refs. [26–30,42]. For the nuclear part of the nucleus-nucleus potential, a double-folding formalism with a Skyrme-type density-dependent effective nucleon-nucleon interaction is used. The parameters of the nucleus-nucleus interaction potential $V(R)$ are adjusted to describe the experimental data at energies above the Coulomb barrier corresponding to spherical nuclei. With this approach many heavy-ion capture reactions at energies above and well below the Coulomb barrier have been successfully described [26–30,42].

Following the hypothesis of Ref. [4], we assume that the sub-barrier capture in the reactions under consideration mainly depends on a $2n$ transfer with a positive Q_{2n} value. Our assumption is that, just before the projectile is captured by the target nucleus (just before the crossing of the Coulomb barrier), which is a slow process, the $2n$ transfer ($Q_{2n} > 0$) occurs and leads to the population of the first-excited collective state in the recipient nucleus [43] (the donor nucleus remains in the ground state). The absolute values of the quadrupole deformation parameters β_2 in the 2^+ state of even-even deformed nuclei are taken from Ref. [44]. For the nuclei deformed in the ground state, the β_2 in the first-excited collective state is similar to that in the ground state. For the double-magic and semimagic nuclei, we take $\beta_2 = 0$ in the ground state.

The motion to N/Z equilibrium starts in the system before the capture occurs because it is energetically favorable in the dinuclear system in the vicinity of the Coulomb barrier. For the reactions under consideration, the average change of mass asymmetry is related to the $2n$ transfer. In these reactions, $Q_{2n} > Q_{1n}$ and during the capture $2n$ transfer is more probable than $1n$ transfer. After the $2n$ transfer the mass numbers, the deformation parameters of the interacting nuclei, and, correspondingly, the height V_b and shape of the Coulomb barrier change. Then one can expect an enhancement or suppression of the capture. If after the neutron transfer the deformations of interacting nuclei increase (decrease), the capture probability increases (decreases). If after the transfer the deformations of interacting nuclei do not change, there is no effect of the neutron transfer on the capture. This scenario has been verified in the description of many reactions [26–30,42].

In Fig. 4 one can see a good agreement between the calculated and the experimental capture cross sections in the reactions ^{40}Ca + ^{94,96}Zr with the positive Q values for neutron transfer and in the reactions ^{40}Ca + ^{90}Zr and ^{48}Ca + ^{90,96}Zr with negative Q values for neutron transfer. The theoretical calculations describe the strong deviation of the slopes of excitation functions in the reactions ^{40}Ca + ^{94,96}Zr with positive Q values for neutron transfer from those in the reactions ^{40}Ca + ^{90}Zr and ^{48}Ca + ^{90,96}Zr, where the neutron transfers are suppressed because of negative Q values (see Fig. 1). This means that the observed capture enhancements in the reactions ^{40}Ca + ^{94,96}Zr at sub-barrier energies are

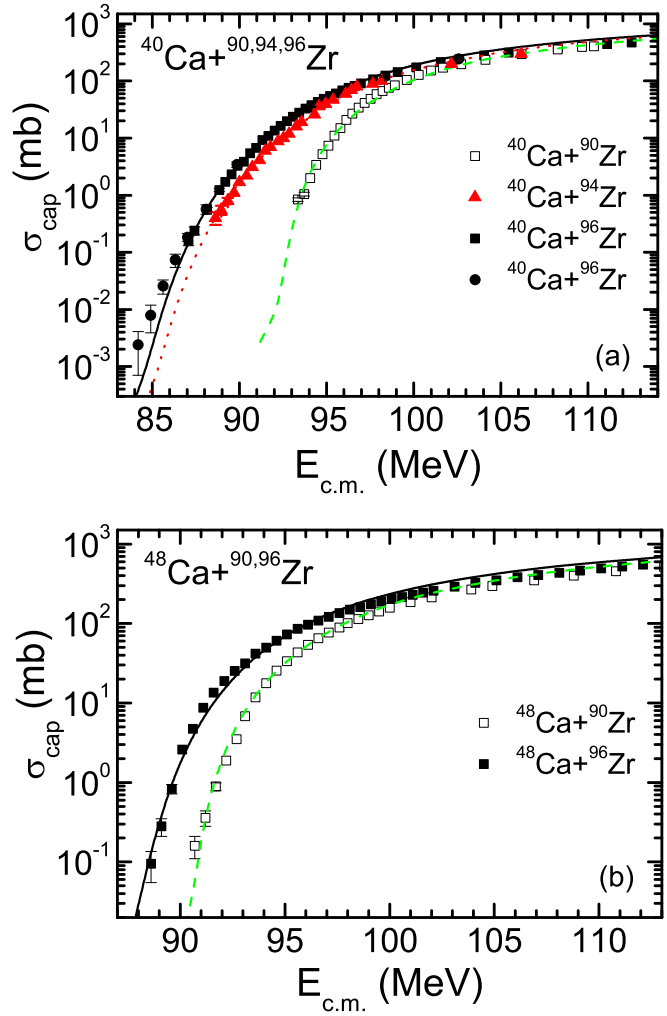

FIG. 4. (Color online) The calculated capture cross sections vs $E_{\text{c.m.}}$ for the reactions (a) ^{40}Ca + ^{96}Zr (solid line), ^{40}Ca + ^{94}Zr (dotted line), and ^{40}Ca + ^{90}Zr (dashed line) and (b) ^{48}Ca + ^{96}Zr (solid line) and ^{48}Ca + ^{90}Zr (dashed line). The error bars are shown if they are larger than the size of the symbols. The experimental data (symbols) are from Refs. [5–7,34].

TABLE II. The configurations before and after two-neutron transfer and the Q_{2n} values for two-neutron transfer in the different reactions.

Reactions with $2n$ transfer	Q_{2n} (MeV)
^{40}Ca($\beta_2 = 0$) + ^{94}Zr($\beta_2 = 0.09$)→^{42}Ca($\beta_2 = 0.25$) + ^{92}Zr($\beta_2 = 0.1$)	4.9
^{40}Ca($\beta_2 = 0$) + ^{96}Zr($\beta_2 = 0.08$)→^{42}Ca($\beta_2 = 0.25$) + ^{94}Zr($\beta_2 = 0.09$)	5.5
^{32}S($\beta_2 = 0.31$) + ^{94}Zr($\beta_2 = 0.09$)→^{34}S($\beta_2 = 0.25$) + ^{92}Zr($\beta_2 = 0.1$)	5.1
^{32}S($\beta_2 = 0.31$) + ^{96}Zr($\beta_2 = 0.08$)→^{34}S($\beta_2 = 0.25$) + ^{94}Zr($\beta_2 = 0.09$)	5.7

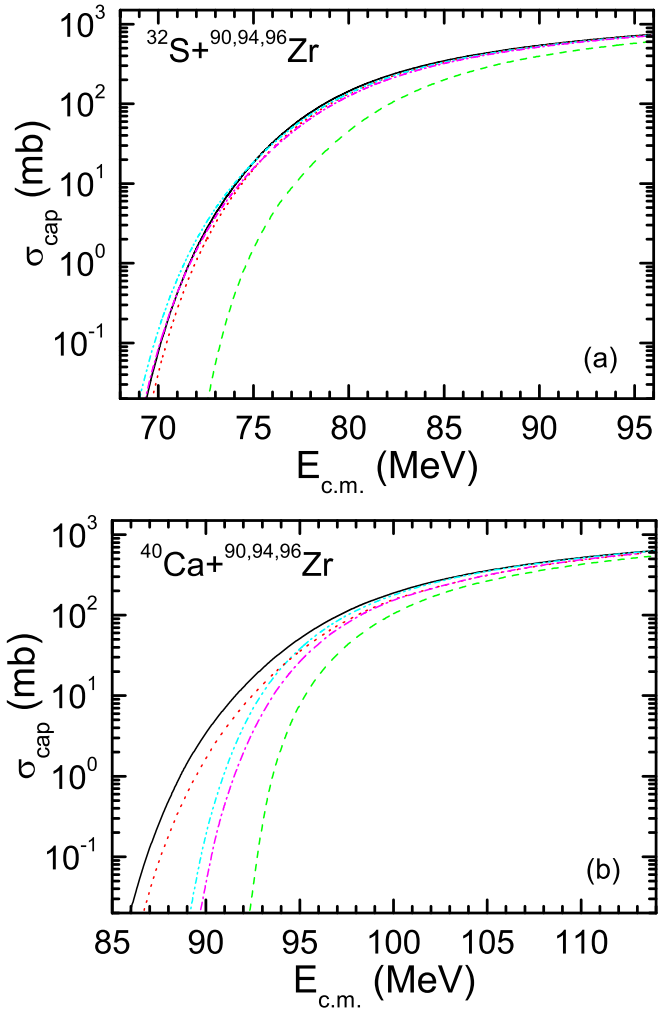

FIG. 5. (Color online) The calculated capture cross sections vs $E_{\mathrm{c.m.}}$ for the reactions (b) ^{40}Ca + ^{96}Zr (solid line), ^{40}Ca + ^{94}Zr (dotted line), and ^{40}Ca + ^{90}Zr (dashed line) and (a) ^{32}S + ^{96}Zr (solid line), ^{32}S + ^{94}Zr (dotted line), and ^{32}S + ^{90}Zr (dashed line). For the reactions ^{32}S,^{40}Ca + ^{96}Zr and ^{32}S,^{40}Ca + ^{94}Zr, the capture cross sections calculated without taking into consideration the neutron transfer are shown by dash-dot-dotted and dash-dotted [it is matched with the solid line in part (a)] lines, respectively.

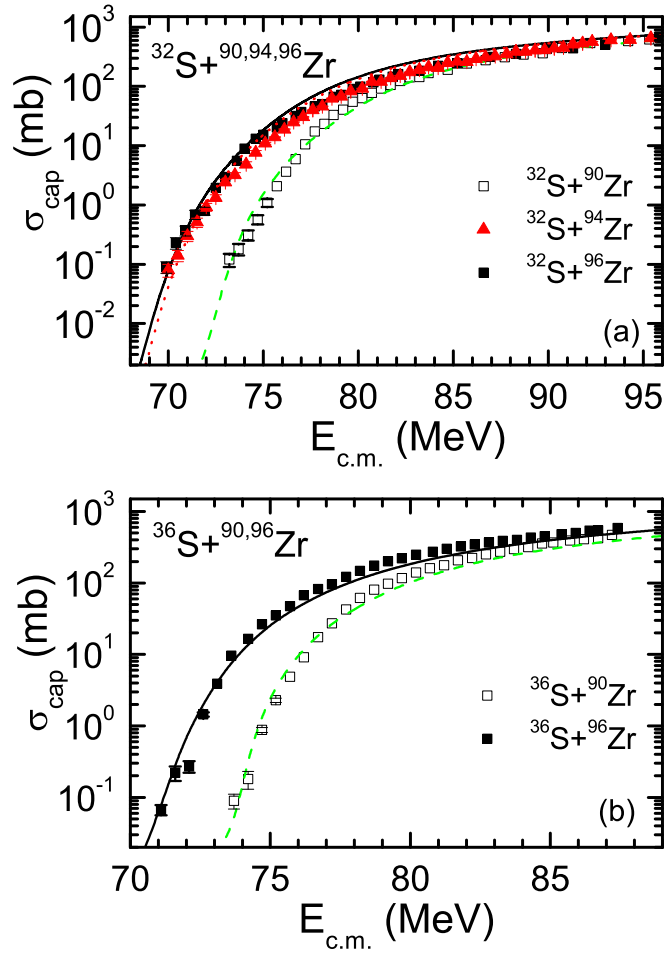

FIG. 6. (Color online) The calculated capture cross sections vs $E_{\mathrm{c.m.}}$ for the reactions (a) ^{32}S + ^{96}Zr (solid line), ^{32}S + ^{94}Zr (dotted line), and ^{32}S + ^{90}Zr (dashed line) and (b) ^{36}S + ^{96}Zr (solid line) and ^{36}S + ^{90}Zr (dashed line). The error bars are shown if they are larger than the size of the symbols. The experimental data (symbols) are from Refs. [18,20,35].

related to the two-neutron transfer effect. After $2n$ transfer in the reactions ^{40}Ca + ^{94,96}Zr the deformation of the light nucleus strongly increases (see Table II) and, thus, the height of the Coulomb barrier decreases for some orientations and the capture cross section becomes larger at smaller $E_{\mathrm{c.m.}}$ (Fig. 4). In Fig. 4 one can see that the sub-barrier fusion (capture) cross section falls down from 10 to 1 mb at ∼1.5 MeV for the reactions ^{48}Ca + ^{90,96}Zr and ^{40}Ca + ^{90}Zr and at about 3 MeV for the reactions ^{40}Ca + ^{94,96}Zr. So, because of the neutron-transfer effect the reactions ^{40}Ca + ^{94,96}Zr show large sub-barrier enhancements with respect to the reactions ^{48}Ca + ^{90,96}Zr and ^{40}Ca + ^{90}Zr (see Figs. 1 and 4). One can see in Fig. 5 that with decreasing the sub-barrier energy the cross sections calculated with and without $2n$ transfer strongly deviate. The slopes of the excitation functions in the reactions ^{40}Ca + ^{94,96}Zr are rather close because in both cases after the neutron transfer the nuclei have similar deformations. The relative enhancement of the sub-barrier fusion cross sections in the reactions ^{40}Ca + ^{94,96}Zr with respect to those in the reactions ^{48}Ca + ^{90,96}Zr and ^{40}Ca + ^{90}Zr is mainly related to the deformation of ^{42}Ca in the 2^+ state. Thus, the observed capture enhancement at sub-barrier energies in the reactions ^{40}Ca + ^{94,96}Zr is purely related to the transfer effects.

Because the sub-barrier enhancements are surprisingly similar for the two reactions ^{40}Ca + ^{94,96}Zr with different positive Q values for neutron transfer, one can assume that the absolute value of the positive Q value is rather unimportant for the capture following transfer. If the transfer is energetically favorable it occurs during the capture process. In this case the transfer influences the capture (fusion) through the change of the isotopic composition of interacting nuclei and, correspondingly, through the change of their deformations.

Figure 6 shows the capture (fusion) excitation functions for the reactions ^{32}S + ^{90,94,96}Zr and ^{36}S + ^{90,96}Zr. The Q_{2n} values for the $2n$-transfer processes are positive (negative) for the

reactions $^{32}S + ^{94,96}Zr$ ($^{32}S + ^{90}Zr$ and $^{36}S + ^{90,96}Zr$). After the $2n$ transfer (before the capture) in the reactions $^{32}S + ^{94,96}Zr$ (Figs. 4 and 6) the deformation of S slightly decreases (see Table II) and the values of the corresponding Coulomb barriers slightly increase. As a result, the transfer weakly suppresses the capture process at the sub-barrier energies. This suppression becomes stronger with decreasing energy. One can see in Fig. 5 that at energies above, near, and below the Coulomb barrier the cross sections with and without $2n$ transfer are almost similar in the reactions $^{32}S + ^{94,96}Zr$. The relative enhancement of the sub-barrier fusion cross sections in the reactions $^{32}S + ^{94,96}Zr$ with respect to that in the reactions $^{36}S + ^{90,96}Zr$ is mainly related to the deformation of ^{34}S in the 2^+ state. With respect to the reactions $^{36}S + ^{94,96}Zr$ the enhancements of cross sections in the reactions $^{32}S + ^{94,96}Zr$ and $^{32}S + ^{90}Zr$ are similar because of the close deformations of interacting nuclei after neutron transfer. Therefore, the observed capture enhancement at sub-barrier energies in the reactions $^{32}S + ^{94,96}Zr$ and $^{32}S + ^{90}Zr$ is not related to the transfer effects but rather to the direct static deformation effects.

The barrier distribution is defined as

$$D(E_{\text{c.m.}}) = d^2[E_{\text{c.m.}}\sigma_{\text{cap}}(E_{\text{c.m.}})]/dE^2_{\text{c.m.}}. \quad (4)$$

In Fig. 7, the distributions D are extracted from the experimental and theoretical excitation functions employing the point-difference approximation [5]:

$$D(E_{\text{c.m.}}) \approx \frac{2E_{\text{c.m.}}\sigma_{\text{cap}}(E_{\text{c.m.}}) - E_{\text{c.m.}}\sigma_{\text{cap}}(E_{\text{c.m.}} + \Delta E_{\text{c.m.}}) - E_{\text{c.m.}}\sigma_{\text{cap}}(E_{\text{c.m.}} - \Delta E_{\text{c.m.}})}{(\Delta E_{\text{c.m.}})^2}. \quad (5)$$

It is clear that with a small energy step $\Delta E_{\text{c.m.}}$ one can approximate the analytical derivative better. However, a large $\Delta E_{\text{c.m.}}$ reduces the experimental uncertainty of D [5]. In Fig. 7, the barrier distribution is extracted with Eq. (5) for two values of $\Delta E_{\text{c.m.}}$, 1.75 and 4.9 MeV.

In Fig. 7, the calculated barrier distribution D has one well-pronounced maximum at $E_{\text{c.m.}} = V_b$ like in the experiments [45] and perfectly fits the experimental data. Without neutron transfer we obtain a narrower barrier distribution for the $^{40}Ca + ^{96}Zr$ reaction. After the $2n$ transfer (before the capture) in the $^{40}Ca + ^{96}Zr$ reaction the deformations of the nuclei increase and, correspondingly, the width of the barrier distribution increases. This leads to the decrease or increase of the Coulomb barrier for the mutual orientations of deformed interacting nuclei. The tip-tip collision has the lowest Coulomb barrier, while the side-side collision results in its highest value. However, the average height of the Coulomb barrier remains the same and approximately corresponds to the Coulomb barrier for the spherical nuclei. Thus, the increase of the deformations of colliding nuclei causes a larger width of barrier distribution. If $E_{\text{c.m.}}$ is lower than the height of the Coulomb barrier at any orientation of colliding nuclei, an increase of their deformations due to the neutron transfer could result in the Coulomb barriers for some orientations that are lower than $E_{\text{c.m.}}$. This leads to fusion enhancement at this $E_{\text{c.m.}}$.

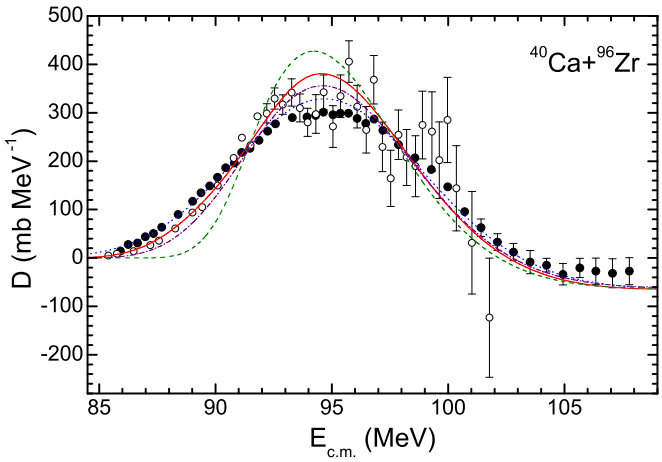

FIG. 7. (Color online) The calculated (lines) and experimental (symbols) fusion barrier distributions D [Eq. (5)] for the $^{40}Ca + ^{96}Zr$ reaction. The solid (dashed) (the energy increment is 1.75 MeV) and dotted (dash-dotted) (the energy increment is 4.9 MeV) lines show the values of D calculated with (without) taking neutron transfer into consideration. The solid (the energy increment is 4.9 MeV) and open (the energy increment is 1.75 MeV) circles are extracted from the experimental excitation function [5].

Note that the extracted values of D are very sensitive to the error bars in σ_{cap}. These error bars and their dependence on energy perhaps create random deviations of experimental points from the calculated curves at $E_{\text{c.m.}} > V_b$ in Fig. 7.

V. SUMMARY

The quantum diffusion approach, the universal fusion function representation, and the extracted capture probabilities from the experimental excitation functions are applied to study the role of neutron transfer with positive Q_{xn} values in the capture (fusion) reactions $^{40}Ca + ^{94,96}Zr$ and $^{32}S + ^{94,96}Zr$. We found that the change of the capture (fusion) cross section after the $2n$ transfer occurs due to the change of the deformations of nuclei. When after the neutron transfer the deformations of nuclei strongly (weakly) change, the neutron transfer strongly (weakly) influences the fusion cross section. We clearly showed that the neutron-transfer effects on the excitation functions in the reactions $^{40}Ca + ^{94,96}Zr$ and $^{32}S + ^{94,96}Zr$ are completely different. The calculations pointed to a strong increase of the fusion enhancement due to the neutron transfer for the systems with the spherical acceptor nuclei like in the case of the reactions $^{40}Ca + ^{94,96}Zr$. In the reactions $^{32}S + ^{94,96}Zr$ with the well-deformed acceptor nucleus ^{32}S, the strong fusion enhancement arises due to the static deformation effects.

ACKNOWLEDGMENTS

We are grateful to C. J. Lin and A. M. Stefanini for providing us with their experimental data. G.G.A. and N.V.A. acknowledge the partial support from the Alexander von Humboldt-Stiftung (Bonn). This work was supported by the RFBR and the NSFC. The IN2P3 (France)-JINR (Dubna) Cooperation Programme is gratefully acknowledged.

[1] L. F. Canto, P. R. S. Gomes, R. Donangelo, and M. S. Hussein, Phys. Rep. **424**, 1 (2006), and references therein.

[2] B. B. Back, H. Esbensen, C. L. Jiang, and K. E. Rehm, Rev. Mod. Phys. **86**, 317 (2014), and references therein.

[3] M. Beckerman *et al.*, Phys. Rev. Lett. **45**, 1472 (1980); M. Beckerman, J. Ball, H. Enge, M. Salomaa, A. Sperduto, S. Gazes, A. DiRienzo, and J. D. Molitoris, Phys. Rev. C **23**, 1581 (1981); M. Beckerman, M. Salomaa, A. Sperduto, J. D. Molitoris, and A. DiRienzo, *ibid.* **25**, 837 (1982).

[4] R. A. Broglia, C. H. Dasso, S. Landowne, and A. Winther, Phys. Rev. C **27**, 2433 (1983); R. A. Broglia, C. H. Dasso, S. Landowne, and G. Pollarolo, Phys. Lett. B **133**, 34 (1983).

[5] H. Timmers *et al.*, Nucl. Phys. A **633**, 421 (1998); Phys. Lett. B **399**, 35 (1997).

[6] A. M. Stefanini *et al.*, Phys. Rev. C **76**, 014610 (2007).

[7] A. M. Stefanini *et al.*, Phys. Lett. B **728**, 639 (2014).

[8] F. Scarlassara *et al.*, Nucl. Phys. A **672**, 99 (2000).

[9] J. J. Kolata *et al.*, Phys. Rev. C **85**, 054603 (2012).

[10] R. Pengo *et al.*, Nucl. Phys. A **411**, 255 (1983).

[11] W. Henning, F. L. H. Wolfs, J. P. Schiffer, and K. E. Rehm, Phys. Rev. Lett. **58**, 318 (1987).

[12] P. H. Stelson, H. J. Kim, M. Beckerman, D. Shapira, and R. L. Robinson, Phys. Rev. C **41**, 1584 (1990).

[13] R. B. Roberts *et al.*, Phys. Rev. C **47**, R1831 (1993).

[14] A. M. Stefanini *et al.*, Phys. Rev. C **52**, R1727 (1995).

[15] A. A. Sonzogni, J. D. Bierman, M. P. Kelly, J. P. Lestone, J. F. Liang, and R. Vandenbosch, Phys. Rev. C **57**, 722 (1998).

[16] V. Tripathi *et al.*, Phys. Rev. C **65**, 014614 (2001).

[17] C. L. Jiang *et al.*, Phys. Rev. C **82**, 041601(R) (2010).

[18] H. Q. Zhang *et al.*, Phys. Rev. C **82**, 054609 (2010).

[19] Z. Kohley *et al.*, Phys. Rev. C **87**, 064612 (2013).

[20] H. M. Jia *et al.*, Phys. Rev. C **89**, 064605 (2014).

[21] P. Jacobs, Z. Fraenkel, G. Mamane, and L. Tserruya, Phys. Lett. B **175**, 271 (1986).

[22] F. Scarlassara *et al.*, EPJ Web Conf. **17**, 05002 (2011).

[23] Z. Kohley *et al.*, Phys. Rev. Lett. **107**, 202701 (2011); J. F. Liang, EPJ Web Conf. **17**, 02002 (2011); J. F. Liang, D. Shapira, C. J. Gross, R. L. Varner, J. R. Beene, P. E. Mueller, and D. W. Stracener, Phys. Rev. C **78**, 047601 (2008).

[24] H. M. Jia *et al.*, Phys. Rev. C **86**, 044621 (2012).

[25] C. L. Jiang, K. E. Rehm, B. B. Back, H. Esbensen, R. V. F. Janssens, A. M. Stefanini, and G. Montagnoli, Phys. Rev. C **89**, 051603(R) (2014).

[26] V. V. Sargsyan, G. G. Adamian, N. V. Antonenko, and W. Scheid, Eur. Phys. J. A **45**, 125 (2010); V. V. Sargsyan, G. G. Adamian, N. V. Antonenko, W. Scheid, and H. Q. Zhang, *ibid.* **47**, 38 (2011); J. Phys.: Conf. Ser. **282**, 012001 (2011); EPJ Web Conf. **17**, 04003 (2011); V. V. Sargsyan, G. G. Adamian, N. V. Antonenko, W. Scheid, C. J. Lin, and H. Q. Zhang, Phys. Rev. C **85**, 017603 (2012); V. V. Sargsyan, G. G. Adamian, N. V. Antonenko, W. Scheid, and H. Q. Zhang, *ibid.* **85**, 037602 (2012).

[27] V. V. Sargsyan, G. G. Adamian, N. V. Antonenko, W. Scheid, and H. Q. Zhang, Phys. Rev. C **84**, 064614 (2011); **85**, 024616 (2012).

[28] V. V. Sargsyan, G. G. Adamian, N. V. Antonenko, W. Scheid, and H. Q. Zhang, Phys. Rev. C **86**, 014602 (2012).

[29] V. V. Sargsyan, G. G. Adamian, N. V. Antonenko, W. Scheid, and H. Q. Zhang, Eur. Phys. J. A **49**, 54 (2013).

[30] V. V. Sargsyan, G. Scamps, G. G. Adamian, N. V. Antonenko, and D. Lacroix, Phys. Rev. C **88**, 064601 (2013).

[31] V. A. Rachkov, A. V. Karpov, A. S. Denikin, and V. I. Zagrebaev, Phys. Rev. C **90**, 014614 (2014).

[32] L. F. Canto, P. R. S. Gomes, J. Lubian, L. C. Chamon, and E. Crema, J. Phys. G **36**, 015109 (2009).

[33] L. F. Canto, P. R. S. Gomes, J. Lubian, L. C. Chamon, and E. Crema, Nucl. Phys. A **821**, 51 (2009).

[34] A. M. Stefanini *et al.*, Phys. Rev. C **73**, 034606 (2006).

[35] A. M. Stefanini *et al.*, Phys. Rev. C **62**, 014601 (2000).

[36] G. Montagnoli *et al.*, Phys. Rev. C **85**, 024607 (2012).

[37] R. A. Broglia, G. Pollarolo, and A. Winther, Nucl. Phys. A **361**, 307 (1981).

[38] C. C. Mahaux, H. Ngô, and G. R. Satchler, Nucl. Phys. A **449**, 354 (1986); G. R. Satchler, Phys. Rep. **199**, 147 (1991).

[39] W. Reisdorf, J. Phys. G: Nucl. Part. Phys. **20**, 1297 (1994).

[40] A. B. Balantekin, S. E. Koonin, and J. W. Negele, Phys. Rev. C **28**, 1565 (1983); A. B. Balantekin and P. E. Reimer, *ibid.* **33**, 379 (1986); A. B. Balantekin, A. J. DeWeerd, and S. Kuyucak, *ibid.* **54**, 1853 (1996).

[41] P. Henrici, *Essentials of Numerical Analysis* (Wiley & Sons, New York, 1982).

[42] R. A. Kuzyakin, V. V. Sargsyan, G. G. Adamian, N. V. Antonenko, E. E. Saperstein, and S. V. Tolokonnikov, Phys. Rev. C **85**, 034612 (2012).

[43] S. Szilner *et al.*, Phys. Rev. C **76**, 024604 (2007); **84**, 014325 (2011).

[44] S. Raman, C. W. Nestor, Jr., and P. Tikkanen, At. Data Nucl. Data Tables **78**, 1 (2001).

[45] A. M. Stefanini *et al.*, Phys. Rev. C **81**, 037601 (2010); **82**, 014614 (2010).